AGU PUBLICATIONS

Geophysical Research Letters

RESEARCH LETTER

10.1002/2017GL074355

**Key Points:**
- Nitrite addition stimulated nitrite oxidation in both oxic and anoxic waters
- Natural assemblages of marine nitrite-oxidizing bacteria have high affinity for nitrite
- Addition of oxygen at μM-level inhibited nitrite oxidation in oxygen depleted waters

**Supporting Information:**
- Supporting Information S1

**Correspondence to:**
X. Sun,
xins@princeton.edu

**Citation:**
Sun, X., Q. Ji, A. Jayakumar, and B. B. Ward (2017), Dependence of nitrite oxidation on nitrite and oxygen in low-oxygen seawater, *Geophys. Res. Lett.*, *44*, 7883–7891, doi:10.1002/2017GL074355.

Received 21 JUN 2017
Accepted 25 JUL 2017
Accepted article online 28 JUL 2017
Published online 12 AUG 2017



# Dependence of nitrite oxidation on nitrite and oxygen in low-oxygen seawater

**Xin Sun[1], Qixing Ji[1,2], Amal Jayakumar[1], and Bess B. Ward[1]**

[1]Department of Geosciences, Princeton University, Princeton, New Jersey, USA, [2]Now at GEOMAR Helmholtz Centre for Ocean Research, Kiel, Germany

**Abstract** Nitrite oxidation is an essential step in transformations of fixed nitrogen. The physiology of nitrite oxidizing bacteria (NOB) implies that the rates of nitrite oxidation should be controlled by concentration of their substrate, nitrite, and the terminal electron acceptor, oxygen. The sensitivities of nitrite oxidation to oxygen and nitrite concentrations were investigated using $^{15}N$ tracer incubations in the Eastern Tropical North Pacific. Nitrite stimulated nitrite oxidation under low in situ nitrite conditions, following Michaelis-Menten kinetics, indicating that nitrite was the limiting substrate. The nitrite half-saturation constant ($K_s = 0.254 \pm 0.161$ μM) was 1–3 orders of magnitude lower than in cultivated NOB, indicating higher affinity of marine NOB for nitrite. The highest rates of nitrite oxidation were measured in the oxygen depleted zone (ODZ), and were partially inhibited by additions of oxygen. This oxygen sensitivity suggests that ODZ specialist NOB, adapted to low-oxygen conditions, are responsible for apparently anaerobic nitrite oxidation.

**Plain Language Summary** Nitrite is a key intermediate in the biogeochemistry of low-oxygen marine environments, including the loss of fixed nitrogen as dinitrogen gas and nitrous oxide. Nitrate reduction to nitrite coupled to reoxidation of nitrite to nitrate has been proposed as a cycle that can preserve bioavailable nitrogen in oxygen minimum zones. This cycle implies that nitrite oxidation occurs in the absence, or near absence, of oxygen. Nitrite oxidation is considered to be an obligately aerobic process, although it has been reported from anoxic waters. Here we report on the regulation of nitrite oxidation by oxygen and nitrite in natural assemblages from the oxygen minimum zone of the Eastern Tropical North Pacific. We show that natural assemblages have very high affinity for nitrite and that oxygen actually inhibits nitrite oxidation in anoxic samples. These findings have implications for the marine nitrogen budget now and in future scenarios of changing ocean conditions.

## 1. Introduction

Nitrogen (N) is an essential nutrient for organisms on Earth. N limits primary production in many parts of the ocean and thus plays an important role in controlling $CO_2$ uptake by the ocean. All N transformations, including the net loss of fixed N, occur in oxygen minimum zones (OMZs) due to the coexistence of oxic and anoxic environments. OMZs are characterized by a strong $O_2$ gradient (oxycline) overlying a layer of high nitrite ($NO_2^-$) concentration coinciding with an oxygen-depleted zone (ODZ) where $O_2$ concentration is low enough to induce anaerobic processes. OMZs are "hot spots" of N loss [*Codispoti*, 1995; *Gruber and Sarmiento*, 1997; *Ulloa et al.*, 2012] via denitrification and anammox [*Ward et al.*, 2009; *Lam and Kuypers*, 2011; *Babbin et al.*, 2014]. Three major OMZs, the Eastern Tropical North Pacific (ETNP), the Eastern Tropical South Pacific (ETSP), and the Arabian Sea, all together contain less than 1% of global seawater in volume but are responsible for up to 30% of N loss in the ocean [*Codispoti et al.*, 2001]. The global expansion of OMZs that is predicted to result from global warming stresses the importance of understanding the N budget in these regions [*Stramma et al.*, 2008].

In addition to N loss transformations, the upper boundaries of the ODZ layers are also sites of intense N cycling, linking aerobic (e.g., nitrification) and anaerobic processes across the oxycline. Even in the core of the ODZ, where $O_2$ is undetectable, nitrifying microbes have been detected [*Lam et al.*, 2009; *Newell et al.*, 2011; *Beman et al.*, 2012; *Peng et al.,* 2013]. The first step of nitrification, ammonium oxidation, could be detected at $O_2$ concentration of 6 nM [*Bristow et al.*, 2016] but has not been detected at apparently anoxic ODZ depths [*Lam et al.*, 2009; *Newell et al.*, 2011; *Peng et al.*, 2016]. There are multiple reports of $NO_2^-$ oxidation at depths where $O_2$ is apparently absent [*Lipschultz et al.*, 1990; *Füssel et al.*, 2012; *Kalvelage et al.*, 2013; *Peng et al.*, 2016]. This means that $NO_2^-$ is not only being reduced to gaseous N in OMZs, but is also being

oxidized into bioavailable nitrate ($NO_3^-$), even in the absence of $O_2$. Anaerobic $NO_2^-$ oxidation to $NO_3^-$ has not been detected in cultivated nitrite oxidizing bacteria (NOB), although some anaerobic metabolism (e.g., $NO_3^-$ reduction) has been demonstrated for the NOB genera, *Nitrobacter* [*Freitag et al.*, 1987] and *Nitrospira* [*Koch et al.*, 2015]. *Nitrospina*, in the newly proposed *Nitrospinae* phylum [*Lücker et al.*, 2013], has been identified as the dominant NOB genus in ODZs [*Beman et al.*, 2013; *Levipan et al.*, 2014; *Ganesh et al.*, 2015] and thus may be the main contributor to apparently anaerobic $NO_2^-$ oxidation. Observations of apparently anaerobic $NO_2^-$ oxidation in the environment are difficult to reconcile with documented metabolic capabilities of known NOB.

To decipher the puzzle of apparently anaerobic $NO_2^-$ oxidation, the controlling factors of the reaction need to be examined. As in other enzyme-catalyzed reactions, the apparent volumetric rate of $NO_2^-$ oxidation is determined by substrate concentration, the catalytic capacity reflected by substrate affinity and the population size of NOB (equivalent to enzyme concentration). The substrate ($NO_2^-$) dependence of marine $NO_2^-$ oxidation has not been determined, and a very limited number of studies have analyzed the effect of $O_2$ on the reaction. Previous studies conducted in low-oxygen seawater reported that $O_2$ had consistently positive effect on $NO_2^-$ oxidation in samples from different depths [*Bristow et al.*, 2016] or had different effects [*Kalvelage et al.*, 2013; *Bristow et al.*, 2017]. Different depths might have different population sizes or types of NOB [*Füssel et al.*, 2012], which can also influence the apparent $NO_2^-$ oxidation kinetics. In order to control for the population size and type of NOB, it is necessary to examine the effect of $NO_2^-$ and $O_2$ concentrations on $NO_2^-$ oxidation rates within samples from the same depth instead of combining samples from different depths. In this study, we used $^{15}N$ tracer incubation experiments to investigate the depth distribution of $NO_2^-$ oxidation and its dependence on availibilities of $NO_2^-$ and $O_2$ in the OMZ of the ETNP.

## 2. Materials and Methods

### 2.1. Experimental Site, Sample Collection, and Incubation

Seawater was collected from six stations (coastal stations PS1 and 8; offshore stations PS2, PS3, 11, and 14; Figure S1 in the supporting information) in the ETNP in April 2016 on board R/V *Ronald H. Brown* (Cruise ID: RB-16-03). $NO_2^-$ oxidation rate profiles were obtained from stations PS1 and PS2. $NO_2^-$ kinetics experiments were performed at stations PS1, 11, and PS3. Samples from stations 8 and 14 were used for $O_2$ kinetics experiments.

Water samples from each depth were collected into five 60 mL serum bottles using 10 L Niskin bottles on a rosette with a conductivity-temperature-depth profiler (CTD) or using a pump profiling system (PPS). In situ $O_2$ concentration (detection limit 2.1 μM), temperature, pressure, and salinity were recorded during each CTD or PPS cast. $NO_2^-$ and $NO_3^-$ concentrations were measured by standard spectrophotometric methods onboard [*United Nations Educational, Scientific and Cultural Organization*, 1994]. For sampling from Niskins from the CTD casts, serum bottles were filled after overflowing three times to minimize $O_2$ contamination and were sealed with rubber septa and aluminum rings immediately after filling. For PPS sampling, bottles were sealed with septa while submerged under seawater pumped from selected depth to avoid oxygenation from the atmosphere. A helium headspace (3 to 10 mL) was introduced into the bottle to facilitate mixing of tracers and $O_2$ adjustment (see below). $^{15}N$–$NO_2^-$ tracer ($^{15}N/(^{14}N + {}^{15}N)$ = 99 atom %) was injected into all five bottles from the same depth to reach a final concentration of 0.4 μM, except for the $NO_2^-$ kinetics experiments in which the final $^{15}N$–$NO_2^-$ tracer concentration varied: 0.05, 0.1, 0.15, 0.2, 0.4, and 1 μM. For the $O_2$ kinetics experiments, ambient seawater was vigorously shaken and exposed to air to reach $O_2$ saturation. Then 0 to 5.0 mL of $O_2$ saturated seawater was added into serum bottles to achieve final $O_2$ concentrations of 0.03, 0.30, 0.70, 1.39, 2.74, and 6.84 μM in seawater. $O_2$ concentration was calculated assuming equilibrium between the water and the gas phases in serum bottles at the incubation temperature (20°C) [*Garcia and Gordon*, 1992]. A set of five bottles incubated in time series (one bottle as $t_0$, two bottles as $t_1$, and two as $t_2$) was used to determine each single rate. Incubations varied from 15 to 24 h and were carried out in controlled temperature rooms (±3°C of in situ temperatures). Incubations were terminated by adding 0.1 mL saturated mercuric chloride ($HgCl_2$) into each serum bottle. Samples were stored at room temperature (18–22°C) in the dark for less than 8 months until analysis in the laboratory.

### 2.2. Isotope Measurement and Rate Determination

To determine the rate of nitrite oxidation to nitrate, the isotopic composition of $NO_3^-$ in each bottle was measured by the denitrifier method [*Sigman et al.*, 2001; *Weigand et al.*, 2016]. Briefly, *Pseudomonas chlororaphis* (ATCC® 43928™) was cultured and concentrated 7 to 10 times by centrifugation in $NO_3^-$/$NO_2^-$-free medium. To avoid interference of nitrite when using the denitrifier method, $NO_2^-$ was removed from samples with sulfamic acid [*Granger and Sigman*, 2009]. Sulfamic acid treated sample (0.4 mL) was aliquoted into each 20 mL vial with concentrated bacteria (1 mL). $NO_3^-$ in the vials was converted into $N_2O$, which was then measured on a mass spectrometer (Delta $V^{plus}$) to determine the nitrogen isotope composition ($\sigma^{15}N$) [*McIlvin and Casciotti*, 2011].

Because no significant change in nitrate concentrations was observed, and the $^{15}N$ content in nitrate samples are low, $[NO_3^-] = [^{14}NO_3^-] + [^{15}NO_3^-] \approx [^{14}NO_3^-]$. Because it is a tracer experiment, the effect of biological fractionation during the incubation experiments is negligible. The nitrite oxidation rate is calculated according to equation (1). $V$ is the nitrite oxidation rate, $F$ is the fraction label of nitrite, and $\frac{d[^{15}NO_3^-]/[^{14}NO_3^-]}{dt}$ is the rate of change of nitrate $^{15}N/^{14}N$, which was determined by the linear regression of time course experiments ($n = 5$). The error bar for each $NO_2^-$ oxidation rate represents the standard error of the slope. The small fraction of $^{15}N$–$NO_3^-$ contamination in the $^{15}N$–$NO_2^-$ tracer [*Peng et al.*, 2015] did not influence the rate calculation because the rate of change in $^{15}N$–$NO_3^-$ over the time course, rather than the absolute value of $^{15}N$–$NO_3^-$ at the endpoint, was used to determine the rate.

$$V = \frac{1}{F} \times [NO_3^-] \times \frac{d[^{15}NO_3^-]/[^{14}NO_3^-]}{dt} \quad (1)$$

### 2.3. Kinetics Models and Rate Estimation

We used the Michaelis-Menten model ([*Monod*, 1942], equation (2)) to evaluate the effect of $NO_2^-$ concentration on $NO_2^-$ oxidation rate. $V_m$ is the potential maximum rate of $NO_2^-$ oxidation when $[NO_2^-]$ is not limiting. $K_s$ is the half-saturation constant, the $[NO_2^-]$ at which the $NO_2^-$ oxidation rate ($V$) equals half of $V_m$. Equation (3) was used to characterize the inhibition effect of $O_2$ on $NO_2^-$ oxidation. In equation (3), $m$ is the potential maximum inhibition by $O_2$ and $n$, analogous to half-saturation constant, is the half-inhibition constant, i.e., the concentration of $O_2$ that caused half of the potential maximum inhibition. The rates of $NO_2^-$ oxidation were normalized to the largest measured rate, which is the rate measured under in situ $[O_2]$ ($V_{\text{in situ O2}}$). The curve fitting tool in Matlab was used to fit the two equations to the measured $NO_2^-$ oxidation rates and $NO_2^-$ or $O_2$ concentrations.

$$V = V_m \times \frac{[NO_2^-]}{[NO_2^-] + K_s} \quad (2)$$

$$\frac{V}{V_{\text{in situ } O_2}} = 1 - m \times \frac{[O_2]}{[O_2] + n} \quad (3)$$

The Michaelis-Menten equation (2) was used to predict the potential maximum rates and the in situ rates of $NO_2^-$ oxidation. Assuming a universal catalytic capacity of enzymes (same $K_s$), the potential maximum rate ($V_m$) at each depth was predicted by introducing the measured $NO_2^-$ oxidation rate ($V$), its corresponding total $[NO_2^-]$ (in situ plus tracer addition), and the average half-saturation constant ($K_s$ = 0.254 μM) into equation (2) (Figure 1). The predicted in situ rate was obtained by introducing $V_m$, in situ $[NO_2^-]$ and $K_s$ into equation (2).

## 3. Results

### 3.1. Depth Distribution of $NO_2^-$ Oxidation

$NO_2^-$ oxidation rates were determined at four or five depths at two stations. Depths were chosen to represent features: the upper oxycline, the top of the ODZ, the core of the ODZ, and the lower oxycline. Highest measured $NO_2^-$ oxidation rates at both stations were detected at ODZ depths (where oxygen concentrations were below detection using the Seabird sensor on the CTD; Figure 1). At station PS1, the highest measured

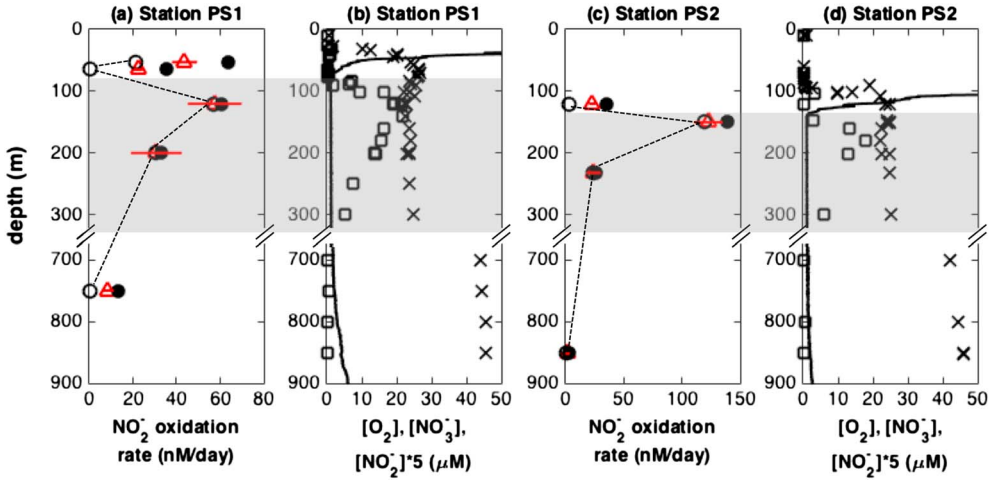


**Figure 1.** Profiles of $NO_2^-$ oxidation rates and $O_2$, $NO_2^-$ and $NO_3^-$ concentrations. Shaded areas indicate ODZs ($[O_2]$ < CTD detection limit). (a, c) Measured rate (red triangle), predicted in situ rate (open circle connected by dashed lines), and predicted maximum rate (filled circle). (b, d) $[O_2]$ (solid line), $[NO_2^-]$ (open square), and $[NO_3^-]$ (cross). Measured rates = slope of linear regression of five independent time course bottles. Error bars = standard error of the regression coefficient.

rate was 57 ± 11.8 nM $d^{-1}$ at the shallower depth in the core of ODZ (120 m). The measured rate (31 ± 11.1 nM $d^{-1}$) at the deeper ODZ depth (200 m) was not significantly different from measured rates at the two oxycline depths. At station PS2, the highest measured rate was 123 ± 11.1 nM $d^{-1}$ in the top of the ODZ (150 m), which was almost 6 times of that at the oxycline depth. The lowest rates at both stations were detected in the lower oxycline.

### 3.2. Effect of $NO_2^-$ on $NO_2^-$ Oxidation Rate

$NO_2^-$ oxidation kinetics were determined by manipulating the $NO_2^-$ concentrations in replicate subsamples from the same Niskin bottle. The relationship between $NO_2^-$ oxidation rates and $NO_2^-$ concentrations in both oxic and anoxic samples with low in situ $NO_2^-$ concentrations (0.1 or 0.05 μM) followed the Michaelis-Menten relationship ([*Monod*, 1942]; equation (2)) with large $r^2$ values (= 0.941 and 0.989, respectively), indicating that $NO_2^-$ was the only limiting substrate in the reaction (Figures 2a and 2b). In other words, the in situ $O_2$ concentration was high enough for the reaction or was not a substrate of the reaction. The rates depend on the physiological characteristics of the NOB and the size of the NOB population, but the half-saturation constant does not depend on population size. The two half-saturation constants (average $K_s$ = 0.254 ± 0.161 μM) from two different stations with different in situ $O_2$ and $NO_2^-$ concentrations were not significantly different, revealing that NOB from these samples had similar high substrate affinity. The $NO_2^-$ oxidation rates increased with increasing $NO_2^-$ concentrations but were not well represented by the Michaelis -Menten relationship when in situ $NO_2^-$ concentration (3.7 μM) was much higher than the $K_s$ (Figure 2c).

The relationship between $NO_2^-$ oxidation rate and substrate concentration was also investigated by plotting $NO_2^-$ oxidation rates measured in the depth profiles (nine depths at stations PS1 and PS2; Figure 1) against the $NO_2^-$ concentration in each incubation (Figure S2). A Michaelis-Menten curve is not suitable to fit these data because they represent rates from samples with different population sizes. The relationship does not intersect zero, although the rate increases with increasing $NO_2^-$ concentration in the oxycline samples, which reinforced the idea that $NO_2^-$ was the limiting substrate of the reaction. $NO_2^-$ oxidation rates at ODZ depths did not show $NO_2^-$ dependence, however, which may imply differences in the size or characteristics of NOB populations in environments with different $O_2$ conditions.

### 3.3. Effect of $O_2$ Concentration on $NO_2^-$ Oxidation Rate

$O_2$ kinetics were assayed in samples from the top of the ODZ, where $O_2$ concentration was below the CTD detection limit and the highest rates of $NO_2^-$ oxidation occurred (Figure 1). Under in situ $O_2$ concentrations,

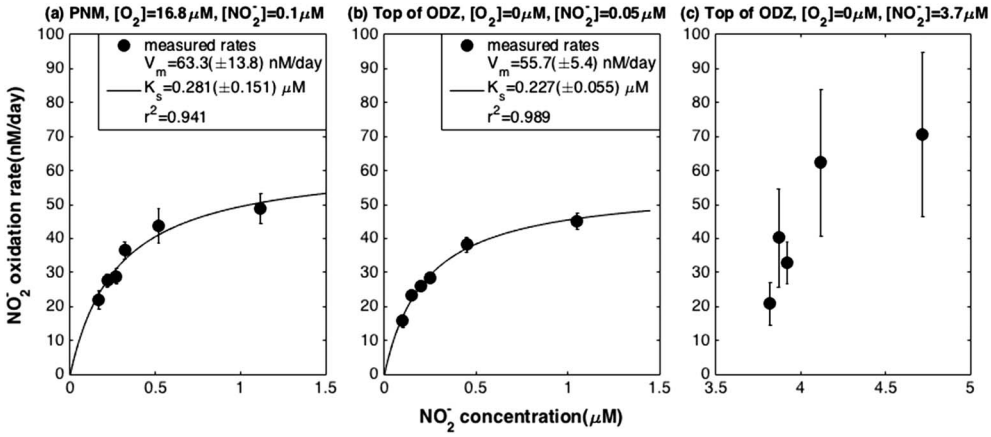


**Figure 2.** $NO_2^-$ dependence of $NO_2^-$ oxidation rates at (a) 53 m at station PS1, (b) 170 m at station PS3, and (c) 130 m at station 11. Measured rates = slope of linear regression of five independent time course bottles. Error bars = standard error of the regression coefficient. Michaelis-Menten equation was fitted to $NO_2^-$ oxidation rates and $NO_2^-$ concentrations in Figures 2a and 2b. Adjusted $r^2$, coefficients ($V_m$ and $K_s$) of the best fit and their 95% confidence intervals are shown in the figure. In situ feature, $[O_2]$ and $[NO_2^-]$ are shown for each figure. PNM = primary nitrite maximum.

nitrite oxidation rates were 143 ± 3.4 and 168 ± 17.9 nM $d^{-1}$ at stations 8 and 14 with total $NO_2^-$ concentrations of 0.43 μM (in situ $[NO_2^-]$ = 0.03 μM) and 1.1 μM (in situ $[NO_2^-]$ = 0.7 μM), respectively. The increased $O_2$ concentrations inhibited $NO_2^-$ oxidation rates following an inhibition curve (Figure 3, equation (3)). At the two stations, the potential maximum inhibitions ($m$) by $O_2$ were 57.3% and 80.1%, respectively. The half-inhibition concentrations ($n$) of $O_2$ were 1.24 and 2.17 μM, respectively.

## 4. Discussion

### 4.1. Effect of $NO_2^-$ on $NO_2^-$ Oxidation Rate

When controlled for population size, $NO_2^-$ kinetics followed the Michaelis-Menten relationship. The half-saturation constant ($K_s$ = 0.254 ± 0.161 μM; average of two experiments, Figure 2) was 1–3 orders of magnitude lower than that of pure cultures of three cultivated NOB genera (*Nitrobacter*, *Nitrotoga*, and *Nitrospira; $K_s$* = 6–544 μM) [*Blackburne et al.*, 2007; *Nowka et al.*, 2015; *Ushiki et al.*, 2017]. $[NO_2^-]$ accumulates to μM levels in OMZs, suggesting that the $K_s$ for $NO_2^-$ might be even lower in regions with lower $[NO_2^-]$. The high affinity of marine NOB (presumably mainly *Nitrospina*-like) for $NO_2^-$ suggests their adaptation to the $NO_2^-$-limited marine environment. This high affinity is analogous to the high affinity for $NH_4^+$ of the natural assemblages of $NH_4^+$-oxidizing microbes [*Horak et al.*, 2013; *Newell et al.*, 2013; *Peng et al.*, 2016], presumably mainly archaea, since high affinity has so far only been observed for the cultivated $NH_4^+$-oxidizing archeon *Nitrosopumilus maritimus* [*Martens-Habbena et al.*, 2009].

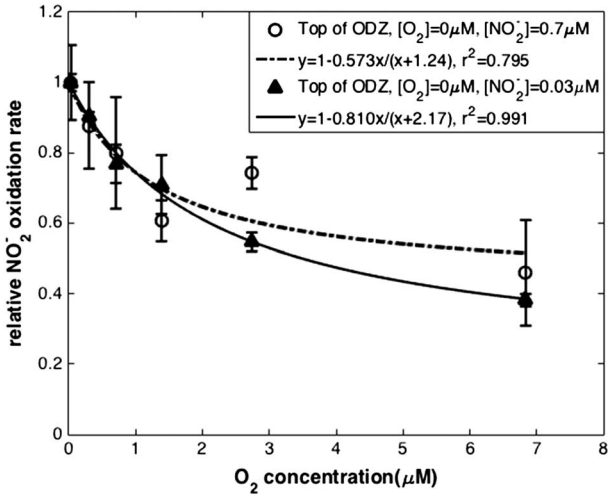


**Figure 3.** $O_2$ dependence of relative $NO_2^-$ oxidation rates at the top of the ODZs. In situ $[O_2]$, $[NO_2^-]$, and the inhibition equations were shown for 89 m at station 8 (filled triangles) and 185 m at station 14 (open circles). Measured rates ($V$) = slope of linear regression of five independent time course bottles. Relative rates = $V/V_{\text{in situ O2}}$. Error bars = standard error of the regression coefficient.

### 4.2. Effect of $O_2$ Concentration on $NO_2^-$ Oxidation Rate

Contrary to expectations for a metabolism that is assumed to require oxygen, increased [$O_2$] consistently inhibited measured $NO_2^-$ oxidation rates. Oxidants other than $O_2$ might also contribute to the $NO_2^-$ oxidation, but all known marine NOB are obligate $O_2$ respirers and use electron transport chains that normally terminate with $O_2$. Anammox bacteria also oxidize $NO_2^-$ anaerobically to $NO_3^-$, during which about 1 mole of $NO_2^-$ is oxidized to $NO_3^-$ per 6 moles of $NO_2^-$ reduced to $N_2$ [*Oshiki et al.*, 2016]. Anammox cannot be the major pathway of apparently anaerobic $NO_2^-$ oxidaton reported here, because measured rates of anammox in this region [*Babbin,* 2014] and in other OMZs [*Hamersley et al.*, 2007; *Dalsgaard et al.*, 2012; *Babbin et al.*, 2014] are much lower (by tenfold) than the $NO_2^-$ oxidation rates reported here.

The decrease in $NO_2^-$ oxidation rates with increasing $O_2$ concentration reported here was not a result of $NO_2^-$ limitation. First, the total $NO_2^-$ concentrations at the top of the ODZ at stations 8 and 14 are much higher than the $K_s$ measured at nearby stations. Second, over the 24 h incubation time, a $NO_2^-$ oxidation rate of 200 nM $d^{-1}$ (larger than any measurement in this study) and a $N_2$ production rate of 60 nM N $d^{-1}$ (larger than any measurement in this region [*Babbin*, 2014]) consume only 0.26 μM of $NO_2^-$, which is much less than the total $NO_2^-$ concentrations in these samples (0.43 μM and 1.1 μM). Therefore, the inhibition of $NO_2^-$ oxidation by $O_2$ was the response of NOB assemblages to $O_2$, independent of $NO_2^-$ concentration.

These samples were collected from depths where $O_2$ was undetectable by the Seabird sensor (<2.1 μM). Previous intercalibrations with the STOX sensor [*Tiano et al.*, 2014] indicated that the true $O_2$ concentration at the sample depths was likely below the STOX sensor detection limits of ~10 nM. Unintended $O_2$ contamination during the sampling process likely occurred [*Revsbech et al.*, 2009], which could have caused uniform low-level contamination of all independent time course samples. This contamination has no effect on the shape of the inhibition curve, showing that $NO_2^-$ oxidation decreased with increasing [$O_2$] at μM level. It does influence, however, determination of the absolute [$O_2$] where the inhibition starts. It is possible that nitrite oxidation is stimulated by increasing [$O_2$] at nM level and saturated at ~1 μM as observed by *Bristow et al.* [2016] with a STOX sensor, but is inhibited by [$O_2$] at μM level.

Sensitivity of NOB from ODZs to $O_2$ is consistent with adaptation to anoxic conditions, such that exposure to μM levels of $O_2$ might cause damage to their cells. This hypothesis is supported by the absence of classical reactive $O_2$ defense mechanisms in *Nitrospina gracilis* isolated from the surface ocean [*Lücker et al.*, 2013]. A previous study found that surface seawater and ODZs had different dominant *Nitrospina* OTUs [*Beman et al.*, 2013]. The present results suggest that ODZ NOB might be low $O_2$ specialists, in having lower $O_2$ tolerance than NOB from oxic environments. Additionally, a metagenomic study from the Arabian Sea found a novel lineage of the gene encoding nitrite oxidoreductase (*nxrA*) that clustered between anammox and *Nitrospina* sequences. This novel *nxrA* sequence was as abundant as *Nitrospina nxrA* at 600 m in the Arabian Sea ODZ [*Lüke et al.*, 2016]. A single-cell genomic study proposed a novel genus within the *Nitrospinae* phylum possessing not only the genetic repertoire for nitrite oxidation but also a nitrate reductase gene [*Ngugi et al.*, 2016]. Nitrite-dependent anaerobic methane oxidizers [*Ettwig et al.*, 2010; *Haroon et al.*, 2013] might oxidize nitrite by reverse reaction of their nitrate reductase enzymes. The nitrate reductase genes are homologous to nitrite oxidoreductase genes. Their contribution to nitrite oxidation in the ODZ, however, is likely to be small due to their low abundance (from undetectable to less than 0.1% of microbial communities) [*Chronopoulou et al.*, 2017; *Padilla et al.*, 2016]. These studies imply that other unidentified organisms, with functional genes homologous to those of anaerobes (i.e., anammox and denitrifiers) might be responsible for apparently anaerobic $NO_2^-$ oxidation.

$O_2$ did not fully inhibit $NO_2^-$ oxidation, i.e., $m < 100\%$, suggesting that parts of the NOB community in the upper ODZ might be similar to surface NOB living in oxic environments (i.e., oxyclines). The apparent percentage of surface NOB in the community varied among different stations. The stimulation of $NO_2^-$ oxidation rate by increasing [$O_2$] at nM level, which was observed in a recent study [*Bristow et al.*, 2016], might be explained by the higher affinity for oxygen of ODZ NOB and a larger proportion of the surface NOB in those samples from the upper oxycline and the ODZ boundary compared to the ODZ samples in this study. *Bristow et al.* [2016] detected a high rate (around 50 nM $d^{-1}$) of $NO_2^-$ oxidation even when ambient $O_2$ was below the STOX sensor detection limit (10 nM), which might be evidence of the presence of ODZ specialist NOB. However, population size and community composition of NOB were not independently controlled in these

samples from three different depths, which might also affect the characterization of $O_2$ kinetics. It is analogous to plotting $NO_2^-$ oxidation rates from multiple samples in this study (Figure S2); the combined data from different depths did not show the [$NO_2^-$] dependence that was evident in experiments in which [$NO_2^-$] and [$O_2$] were independently varied within samples from the same depth.

### 4.3. $NO_2^-$ Oxidation in ODZs and Its Significance

The $NO_2^-$ oxidation rate in ODZs can never be fueled by $O_2$ contamination if there were no NOB in the seawater. The high rates detected in the ODZ in this and other studies [*Lipschultz et al.*, 1990; *Peng et al.*, 2015; *Babbin et al.*, 2017] together with molecular data [*Füssel et al.*, 2012; *Beman et al.*, 2013] directly support the idea that microbes with $NO_2^-$ oxidation capacity were present in the anoxic seawater. Evidence in support of their in situ $NO_2^-$ oxidation activities in ODZs is provided by model simulations [*Buchwald et al.*, 2015] and stable isotope measurements [*Casciotti et al.*, 2013; *Gaye et al.,* 2013; *Peters et al.*, 2016]. The isotopic composition of $NO_2^-$ in the ODZ is relatively $^{15}N$ depleted, which is attributed to the inverse isotope effect during $NO_2^-$ oxidation to $NO_3^-$ [*Casciotti*, 2009].

To evaluate the effect of experimental conditions on measured rates, we used the kinetics data to predict in situ rates and potential maximum rates ($V_m$) (Figure 1). In the core of the ODZs, measured rates were not significantly different from $V_m$ since the total $NO_2^-$ concentrations were much higher than $K_s$. The predicted $V_m$ was a proxy for the size of the NOB population, assuming similar substrate affinity of NOB involved in $NO_2^-$ oxidation (similar $K_s$ determined in $NO_2^-$ kinetics experiments at two depths makes this a reasonable assumption). The predicted $V_m$ varied among depths, indicating the necessity of controlling population size while characterizing $NO_2^-$ or $O_2$ kinetics. The implied population size at the top of the ODZ was much larger than that at any other depth. The implied abundance of NOB at the top of the ODZs might be due to the relatively higher $NO_2^-$ supply, and $O_2$ invasion events may enable the persistence of both ODZ specialist NOB and surface NOB. The inferred population size in the core of the ODZs was of the same magnitude as that in the oxycline. If NOB communities at ODZ depths consist only of surface NOB, which prefer oxic conditions, the puzzle of how they make a living and oxidize $NO_2^-$ in the absence of $O_2$ must be solved. More likely, ODZ specialist NOB are dominant in the core of the ODZ where anoxia is more stable and the assemblage is more isolated from the oxic environment. However, $NO_2^-$ oxidation rates in the core of the ODZ were higher than or similar to rates in surface seawater (Figure 1), implying that ODZ specialist NOB survived in the anoxic environment. One of the potential oxidants for $NO_2^-$ oxidation in the ODZ is iodate; however, iodate alone is insufficient to support the measured rates [*Babbin et al.*, 2017]. Other potential oxidants that might contribute to oxidizing $NO_2^-$ in these anoxic seawaters remain to be identified. Likewise the identity of potential ODZ specialist NOB and whether they are capable of conducting alternative anaerobic reactions (i.e., denitrification) await further exploration.

Regardless of the mechanism of $NO_2^-$ oxidation in the ODZ, high $NO_2^-$ oxidation rates detected in ODZs can be coupled with $NO_3^-$ reduction to constitute an efficient $NO_2^- \longleftrightarrow NO_3^-$ cycle, which preserves bioavailable N in this intense N loss spot [*Füssel et al.*, 2012; *Casciotti et al.*, 2013; *Peters et al.*, 2016]. The $NO_2^- \longleftrightarrow NO_3^-$ cycle may also provide $NH_4^+$ to fuel anammox because $NO_3^-$ is used as an electron acceptor to oxidize organic matter in the absence of oxygen, and thus liberates $NH_4^+$. $NO_3^-$ reduction to $NO_2^-$ is a more widespread metabolic capacity of microbes than complete denitrification ($NO_2^- \rightarrow NO \rightarrow N_2O \rightarrow N_2$), and $NO_3^-$ reduction is the most important anaerobic respiration process in the low oxygen seawater, based on observed rates [*Lipschultz et al.*, 1990; *Lam et al.*, 2009]. Thus, $NO_3^-$ reduction to $NO_2^-$ would provide $NH_4^+$ in excess of that supplied by organic matter remineralization occurring during complete denitrification. A model that included $NO_2^-$ oxidation in the ODZ successfully explained the formation of the secondary $NO_2^-$ maximum [*Babbin et al.*, 2017]. The modeling exercise indicates the necessity of including the recycling between $NO_2^-$ and $NO_3^-$ in the anoxic environment in order to reevaluate the N budget in the ocean, especially the contribution of OMZs to N loss. This reevaluation is also important to predict the response of the N cycle and potential perturbation of the N budget under the expansion of OMZs.

**Acknowledgments**
We gratefully acknowledge the chief scientist, Margaret Mulholland and all crew members of NOAA Ship Ronald H. Brown for assistance. We thank Brittany Widner, Nicole Travis, Matthew Forbes, and Peter Bernhardt for nutrient analysis. We thank Marguerite Blum for assistance of PPS operation. And we thank two anonymous reviewers for their insightful comments. The manuscript is prepared to comply with AGU data policy. Detailed information about the data and method reported here should be addressed to xins@princeton.edu. This research was supported by a first year fellowship from Princeton University to Xin Sun and the National Science Foundation Oceanography awards (1356043) to Amal Jayakumar and Margaret Mulholland.

## References

Babbin, A. R., R. G. Keil, A. H. Devol, and B. B. Ward (2014), Organic matter stoichiometry, flux, and oxygen control nitrogen loss in the ocean, *Science*, *344*(6182), 406–408, doi:10.1126/science.1248364.
Babbin A. R. (2014), Biogeochemical Controls on Fixed Nitrogen Loss Processes in the Marine Environment, PhD dissertation, Princeton Univ.

Babbin, A. R., B. D. Peters, C. W. Mordy, B. Widner, K. L. Casciotti, and B. B. Ward (2017), Multiple metabolisms constrain the anaerobic nitrite budget in the eastern tropical South Pacific, *Global Biogeochem. Cycles*, *31*, 258–271, doi:10.1002/2016GB005407.

Beman, J. M., B. N. Popp, and S. E. Alford (2012), Quantification of ammonia oxidation rates and ammonia-oxidizing archaea and bacteria at high resolution in the Gulf of California and eastern tropical North Pacific Ocean, *Limnol. Oceanogr.*, *57*(3), 711–726, doi:10.4319/lo.2012.57.3.0711.

Beman, J. M., J. L. Shih, and B. N. Popp (2013), Nitrite oxidation in the upper water column and oxygen minimum zone of the eastern tropical North Pacific Ocean, *ISME J.*, *7*(11), 2192–2205, doi:10.1038/ismej.2013.96.

Blackburne, R., V. M. Vadivelu, Z. Yuan, and J. Keller (2007), Kinetic characterisation of an enriched Nitrospira culture with comparison to Nitrobacter, *Water Res.*, *41*(14), 3033–3042, doi:10.1016/j.watres.2007.01.043.

Bristow, L. A., et al. (2016), Ammonium and nitrite oxidation at nanomolar oxygen concentrations in oxygen minimum zone waters, *Proc. Natl. Acad. Sci.*, *113*, doi:10.1073/pnas.1600359113.

Bristow, L. A., et al. (2017), $N_2$ production rates limited by nitrite availability in the bay of Bengal oxygen minimum zone, *Nat. Geosci.*, *10*(1), 24–29, doi:10.1038/ngeo2847.

Buchwald, C., A. E. Santoro, R. H. R. Stanley, and K. L. Casciotti (2015), Nitrogen cycling in the secondary nitrite maximum of the eastern tropical North Pacific off Costa Rica, *Global Biogeochem. Cycles*, *29*, 2061–2081, doi:10.1002/2015GB005187.

Casciotti, K. L. (2009), Inverse kinetic isotope fractionation during bacterial nitrite oxidation, *Geochim. Cosmochim. Acta*, *73*(7), 2061–2076, doi:10.1016/j.gca.2008.12.022.

Casciotti, K. L., C. Buchwald, and M. McIlvin (2013), Implications of nitrate and nitrite isotopic measurements for the mechanisms of nitrogen cycling in the Peru oxygen deficient zone, *Deep Sea Res., Part I*, *80*, 78–93, doi:10.1016/j.dsr.2013.05.017.

Chronopoulou, P., F. Shelley, W. J. Pritchard, S. T. Maanoja, and M. Trimmer (2017), Origin and fate of methane in the eastern tropical North Pacific oxygen minimum zone, *ISME J.*, doi:10.1038/ismej.2017.6.

Codispoti, L. (1995), Is the ocean losing nitrate?, *Nature*, *376*(6543), 724, doi:10.1038/376724a0.

Codispoti, L. A., J. A. Brandes, J. P. Christensen, A. H. Devol, S. W. A. Naqvi, H. W. Paerl, and T. Yoshinari (2001), The oceanic fixed nitrogen and nitrous oxide budgets: Moving targets as we enter the anthropocene?, *Sci. Mar.*, *65*(2), 85–105, doi:10.3989/scimar.2001.65s285.

Dalsgaard, T., B. Thamdrup, L. Farías, and N. P. Revsbech (2012), Anammox and denitrification in the oxygen minimum zone of the eastern South Pacific, *Limnol. Oceanogr.*, *57*(5), 1331–1346, doi:10.4319/lo.2012.57.5.1331.

Ettwig, K. F., et al. (2010), Nitrite-driven anaerobic methane oxidation by oxygenic bacteria, *Nature*, *464*(7288), 543–548, doi:10.1038/nature08883.

Freitag, A., M. Rudert, and E. Bock (1987), Growth of Nitrobacter by dissimilatoric nitrate reduction, *FEMS Microbiol. Lett.*, *48*, 105–109.

Füssel, J., P. Lam, G. Lavik, M. M. Jensen, M. Holtappels, M. Gunter, and M. M. M. Kuypers (2012), Nitrite oxidation in the Namibian oxygen minimum zone, *ISME J.*, *6*, 1200–1209, doi:10.1038/ismej.2011.178.

Ganesh, S., L. A. Bristow, M. Larsen, N. Sarode, B. Thamdrup, and F. J. Stewart (2015), Size-fraction partitioning of community gene transcription and nitrogen metabolism in a marine oxygen minimum zone, *ISME J.*, *9*(12), 2682–2696, doi:10.1038/ismej.2015.44.

Garcia, H. E., and L. I. Gordon (1992), Oxygen solubility in seawater: Better fitting equations, *Limnol. Oceanogr.*, *37*(6), 1307–1312, doi:10.4319/lo.1992.37.6.1307.

Gaye, B., B. Nagel, K. Dähnke, T. Rixen, and K. C. Emeis (2013), Evidence of parallel denitrification and nitrite oxidation in the ODZ of the Arabian Sea from paired stable isotopes of nitrate and nitrite, *Global Biogeochem. Cycles*, *27*, 1059–1071, doi:10.1002/2011GB004115.

Granger, J., and D. M. Sigman (2009), Removal of nitrite with sulfamic acid for nitrate N and O isotope analysis with the denitrifier method, *Rapid Commun. Mass Spectrom.*, *23*, 3753–3762, doi:10.1002/rcm.4307.

Gruber, N., and J. Sarmiento (1997), Global patterns of marine nitrogen fixation and denitrification, *Global Biogeochem. Cycles*, *11*, 235–266, doi:10.1029/97GB00077.

Hamersley, M. R., et al. (2007), Anaerobic ammonium oxidation in the Peruvian oxygen minimum zone, *Limnol. Oceanogr.*, *52*(3), 923–933, doi:10.4319/lo.2007.52.3.0923.

Haroon, M. F., S. Hu, Y. Shi, M. Imelfort, J. Keller, P. Hugenholtz, Z. Yuan, and G. W. Tyson (2013), Anaerobic oxidation of methane coupled to nitrate reduction in a novel archaeal lineage, *Nature*, *500*(7464), 567–570, doi:10.1038/nature12375.

Horak, R. E. A., W. Qin, A. J. Schauer, E. V. Armbrust, A. E. Ingalls, J. W. Moffett, D. A. Stahl, and A. H. Devol (2013), Ammonia oxidation kinetics and temperature sensitivity of a natural marine community dominated by Archaea, *ISME J.*, *7*(10), 2023–2033, doi:10.1038/ismej.2013.75.

Kalvelage, T., G. Lavik, P. Lam, S. Contreras, L. Arteaga, C. R. Loscher, A. Oschlies, A. Paulmier, L. Stramma, and M. M. M. Kuypers (2013), Nitrogen cycling driven by organic matter export in the South Pacific oxygen minimum zone, *Nat. Geosci.*, *6*(3), doi:10.1038/ngeo1739.

Koch, H., S. Lücker, M. Albertsen, K. Kitzinger, C. Herbold, E. Spieck, P. H. Nielsen, M. Wagner, and H. Daims (2015), Expanded metabolic versatility of ubiquitous nitrite-oxidizing bacteria from the genus *Nitrospira*, *Proc. Natl. Acad. Sci.*, *112*(36), 11,371–11,376, doi:10.1073/pnas.1506533112.

Lam, P., and M. M. M. Kuypers (2011), Microbial nitrogen cycling processes in oxygen minimum zones, *Annu. Rev. Mar. Sci.*, *3*(1), 317–345, doi:10.1146/annurev-marine-120709-142814.

Lam, P., G. Lavik, M. M. Jensen, J. van de Vossenberg, M. Schmid, D. Woebken, G. Dimitri, R. Amann, M. S. M. Jetten, and M. M. M. Kuypers (2009), Revising the nitrogen cycle in the Peruvian oxygen minimum zone, *Proc. Natl. Acad. Sci.*, *106*(12), 4752–4757, doi:10.1073/pnas.0812444106.

Levipan, H. A., V. Molina, and C. Fernandez (2014), *Nitrospina*-like bacteria are the main drivers of nitrite oxidation in the seasonal upwelling area of the eastern South Pacific (Central Chile ~36°S), *Environ. Microbiol. Rep.*, *6*(6), 565–573.

Lipschultz, F., S. C. Wofsy, B. B. Ward, L. A. Codispoti, G. Friedrich, and J. W. Elkins (1990), Bacterial transformations of inorganic nitrogen in the oxygen-deficient waters of the eastern tropical South Pacific Ocean, *Deep Sea Res., Part A*, *37*(10), 1513–1541, doi:10.1016/0198-0149(90)90060-9.

Lücker, S., B. Nowka, T. Rattei, E. Spieck, and H. Daims (2013), The genome of *Nitrospina gracilis* illuminates the metabolism and evolution of the major marine nitrite oxidizer, *Front. Microbiol.*, *4*, 1–19, doi:10.3389/fmicb.2013.00027.

Lüke, C., D. R. Speth, M. A. R. Kox, L. Villanueva, and M. S. M. Jetten (2016), Metagenomic analysis of nitrogen and methane cycling in the Arabian Sea oxygen minimum zone, *Peer J.*, *4*, doi:10.7717/peerj.1924.

Martens-Habbena, W., P. M. Berube, H. Urakawa, J. R. de la Torre, and D. A. Stahl (2009), Ammonia oxidation kinetics determine niche separation of nitrifying archaea and bacteria, *Nature*, *461*(7266), 976–979, doi:10.1038/nature08465.

McIlvin, M. R., and K. L. Casciotti (2011), Technical updates to the bacterial method for nitrate isotopic analyses, *Anal. Chem.*, *83*(5), 1850–1856, doi:10.1021/ac1028984.

Monod, J. (1942), *Recherches sur la croissance des cultures bacteriennes*, Hermann & Cie, Paris.

Newell, S. E., A. R. Babbin, A. Jayakumar, and B. B. Ward (2011), Ammonia oxidation rates and nitrification in the Arabian Sea, *Global Biogeochem. Cycles*, *25*, GB4016, doi:10.1029/2010GB003940.

Newell, S. E., S. E. Fawcett, and B. B. Ward (2013), Depth distribution of ammonia oxidation rates and ammonia-oxidizer community composition in the Sargasso Sea, *Limnol. Oceanogr.*, *58*(4), 1491–1500, doi:10.4319/lo.2013.58.4.1491.

Ngugi, D. K., J. Blom, R. Stepanauskas, and U. Stingl (2016), Diversification and niche adaptations of Nitrospina-like bacteria in the polyextreme interfaces of Red Sea brines, *ISME J.*, *10*, 1383–1399, doi:10.1038/ismej.2015.214.

Nowka, B., H. Daims, and E. Spieck (2015), Comparison of oxidation kinetics of nitrite-oxidizing bacteria: Nitrite availability as a key factor in niche differentiation, *Appl. Environ. Microbiol.*, *81*(2), 745–753, doi:10.1128/AEM.02734-14.

Oshiki, M., H. Satoh, and S. Okabe (2016), Ecology and physiology of anaerobic ammonium oxidizing bacteria, *Environ. Microbiol.*, *18*(9), 2784–2796, doi:10.1111/1462-2920.13134.

Padilla, C. C., et al. (2016), NC10 bacteria in marine oxygen minimum zones, *ISME J.*, *10*(8), 2067–2071, doi:10.1038/ismej.2015.262.

Peng, X., A. Jayakumar, and B. B. Ward (2013), Community composition of ammonia-oxidizing archaea from surface and anoxic depths of oceanic oxygen minimum zones, *Front. Microbiol.*, *4*(177), doi:10.3389/fmicb.2013.00177.

Peng, X., C. A. Fuchsman, A. Jayakumar, S. Oleynik, and W. Martens-habbena (2015), Ammonia and nitrite oxidation in the Eastern Tropical North Pacific, *Global Biogeochem. Cycles*, *29*, 2034–2049, doi:10.1002/2015GB005278.

Peng, X., C. A. Fuchsman, A. Jayakumar, M. J. Warner, A. H. Devol, and B. B. Ward (2016), Revisiting nitrification in the eastern tropical South Pacific: A focus on controls, *J. Geophys. Res. Ocean.*, *121*, 1667–1684, doi:10.1002/2015JC011455.

Peters, B. D., A. R. Babbin, K. A. Lettmann, C. W. Mordy, O. Ulloa, B. B. Ward, and K. L. Casciotti (2016), Vertical modeling of the nitrogen cycle in the eastern tropical South Pacific oxygen deficient zone using high-resolution concentration and isotope measurements, *Global Biogeochem. Cycles*, *30*, 1661–1681, doi:10.1002/2016GB005415.

Revsbech, N. P., L. H. Larsen, J. Gundersen, T. Dalsgaard, O. Ulloa, and B. Thamdrup (2009), Determination of ultra-low oxygen concentrations in oxygen minimum zones by the STOX sensor, *Limnol. Oceanogr. Methods*, *7*, 371–381, doi:10.4319/lom.2009.7.371.

Sigman, D. M., K. L. Casciotti, M. Andreani, C. Barford, M. Galanter, and J. K. Böhlke (2001), A bacterial method for the nitrogen isotopic analysis of nitrate in seawater and freshwater, *Anal. Chem.*, *73*(17), 4145–4153, doi:10.1021/ac010088e.

Stramma, L., G. C. Johnson, J. Sprintall, and V. Mohrholz (2008), Expanding oxygen-minimum zones in the tropical oceans, *Science*, *320*(5876), 655–658, doi:10.1126/science.1153847.

Tiano, L., E. Garcia-Robledo, T. Dalsgaard, A. H. Devol, B. B. Ward, O. Ulloa, D. E. Canfield, and N. Peter Revsbech (2014), Oxygen distribution and aerobic respiration in the north and south eastern tropical Pacific oxygen minimum zones, *Deep Sea Res., Part I*, *94*, 173–183, doi:10.1016/j.dsr.2014.10.001.

Ulloa, O., D. E. Canfield, E. F. DeLong, R. M. Letelier, and F. J. Stewart (2012), Microbial oceanography of anoxic oxygen minimum zones, *Proc. Natl. Acad. Sci.*, *109*(40), 15996–16003, doi:10.1073/pnas.1205009109.

United Nations Educational, Scientific and Cultural Organization (1994), Protocols for the Joint GlobalOcean Flux Study (JGOFS) Core Measurements, I. O. Commission, United Nations Educational, Scientific and Cultural Organization.

Ushiki, N., M. Jinno, H. Fujitani, T. Suenaga, A. Terada, and S. Tsuneda (2017), Nitrite oxidation kinetics of two *Nitrospira* strains: The quest for competition and ecological niche differentiation, *J. Biosci. Bioeng.*, *123*(5), 581–589, doi:10.1016/j.jbiosc.2016.12.016.

Ward, B. B., A. H. Devol, J. J. Rich, B. X. Chang, S. E. Bulow, H. Naik, A. Pratihary, and A. Jayakumar (2009), Denitrification as the dominant nitrogen loss process in the Arabian Sea, *Nature*, *461*(7260), 78–81, doi:10.1038/nature08276.

Weigand, M. A., J. Foriel, B. Barnett, S. Oleynik, and D. M. Sigman (2016), Updates to instrumentation and protocols for isotopic analysis of nitrate by the denitrifier method, *Rapid Commun. Mass Spectrom.*, *30*(12), 1365–1383, doi:10.1002/rcm.7570.